Since January 2020 Elsevier has created a COVID-19 resource centre with free information in English and Mandarin on the novel coronavirus COVID-19. The COVID-19 resource centre is hosted on Elsevier Connect, the company's public news and information website.

Severe Acute Respiratory Syndrome Coronavirus 2 Attachment Receptor Angiotensin-Converting Enzyme 2 Is Decreased in Crohn's Disease and Regulated By Microbial and Inflammatory Signaling

Jay Vasant Patankar,[1] Mircea Teodor Chiriac,[1] Malte Lehmann,[2,3] Anja A. Kühl,[2,3,4] Raja Atreya,[1,3,5] and Christoph Becker[1,3]

[1]Department of Medicine 1, University of Erlangen-Nuremberg, Erlangen, Germany; [2]Charité – Universitätsmedizin Berlin, corporate member of Freie Universität Berlin, Humboldt-Universität zu Berlin and Berlin Institute of Health, Medizinische Klinik für Gastroenterologie, Infektiologie und Rheumatologie, Berlin, Germany; [3]The Transregio 241 IBDome Consortium; [4]Charité - Universitätsmedizin Berlin, corporate member of Freie Universität Berlin, Humboldt Universität zu Berlin, and Berlin Institute of Health, iPATH.Berlin, Berlin, Germany; [5]Deutsches Zentrum Immuntherapie (DZI), Erlangen, Germany; [6]Department of Biochemistry, Faculty of Medicine, Medical University of Lodz, Lodz, Poland; [7]College of Veterinary Medicine, Northeast Agricultural University, Harbin, People's Republic of China; and [8]Department of Infection Biology, University Hospital Erlangen, Erlangen, Germany

The disease now known as coronavirus disease 2019 (COVID-19) is caused by a novel beta coronavirus denoted severe acute respiratory syndrome coronavirus 2 (SARS-CoV-2) and was initially reported in December 2019 as pneumonia of unknown cause.[1–4] Recently, it was described that in humans co-expression of angiotensin-converting enzyme 2 (ACE2) and the transmembrane protease serine 2 (TMPRSS2) promotes the entry of SARS-CoV-2 into host cells.[5]

Recent reports suggest that between 6% and 48% of COVID-19 cases experience digestive symptoms with or without diarrhea as their main complaint at presentation or on hospitalization.[6] These patients may have worse clinical outcomes than those with respiratory symptoms alone.[6] Recently, infection of intestinal epithelial cell (IEC) organoids by SARS-CoV-2 was demonstrated,[7] raising concerns for patients with pre-existing chronic intestinal conditions such as inflammatory bowel disease (IBD).

Little is known about the regulation of ACE2 and TMPRSS2 in the gut during inflammation. Previous studies were inconclusive on the levels of ACE2 in IBD.[8] Here, we present collective results on the regulation of intestinal ACE2 and TMPRSS2 in human and experimental models of intestinal inflammation and present data on the putative signaling mechanisms that control their expression via cytokines and pattern recognition receptors in the gut epithelium.

Methods

Patients and Control Subjects

One hundred twenty-nine IBD patients were analyzed across all experiments. The ethics committee of the University Hospital of Erlangen and Charité–University Hospital Berlin approved experiments involving human material.

Mice

C57/Bl6 and Rag2-/- mice were purchased from Charles River Laboratories. Please refer to Supplementary Methods for details on mouse strains, materials, and methods.

Results

Interestingly, ACE2 but not TMPRSS2 expression was substantially lower in inflamed ilea (score 3) of Crohn's disease (CD) patients than uninflamed control subjects (score 0) and correlated negatively with the expression of an established inflammation marker, S100A8 (Figure 1A). Contrary to CD and consistent with previously published datasets, the expression levels of ACE2 and TMPRSS2 remained unchanged in the inflamed colon of ulcerative colitis (UC) patients (Figure S1A and B). Quantitative immunohistochemical analysis revealed a reduction in ACE2 but not TMPRSS2 protein in the inflamed ilea of CD patients but not in the colon of UC patients (Figure 1B and C, Figure S1C). These data show that transcript and protein levels of ACE2 are reduced in inflamed CD ileum.

To systematically investigate how inflammation alters ACE2 and TMPRSS2 expression, we performed RNA sequencing from control and inflamed tissues from multiple well-established mouse models. In all models tested, the expression of Ace2 but not Tmprss2 was downregulated during inflammation (Figure 1D, Figure S1D). Our findings of reduced Ace2 expression in mouse colitis models also corroborated with various stages of inflammation in DSS colitis (Figure S1E) and with previous transcriptomic datasets (Figure S1F). Immunostaining revealed altered localization of IEC ACE2 protein in inflamed tissues, with a progressive cytosolic translocation with increasing inflammation (Figure 1F and insets).

Interferon (IFN) responses are induced during viral infections and in IBD. In our experiment comparing transcriptome-wide responses to IFNs from wild-type,

Most current article

$Stat1^{-/-}$, and $Stat2^{-/-}$ organoids, we observed strong repression of $Ace2$ in response to IFN-β and -λ and of Tmprss2 to IFN-γ (Figure 1G). Interestingly, such suppression was absent in organoids from $Stat1^{-/-}$ mice (Figure 1G). However, the IFN-mediated $Ace2$ downregulation was still apparent in $Stat2^{-/-}$ organoids (Figure 1G). Thus, IFN-mediated $Ace2$ repression in IEC requires STAT1 but not STAT2. Furthermore, expression of intestinal $Ace2$ was repressed in mice overexpressing IFN-λ (Figure 1H). Type 2 immune responses are predominant in UC. Stimulation of intestinal
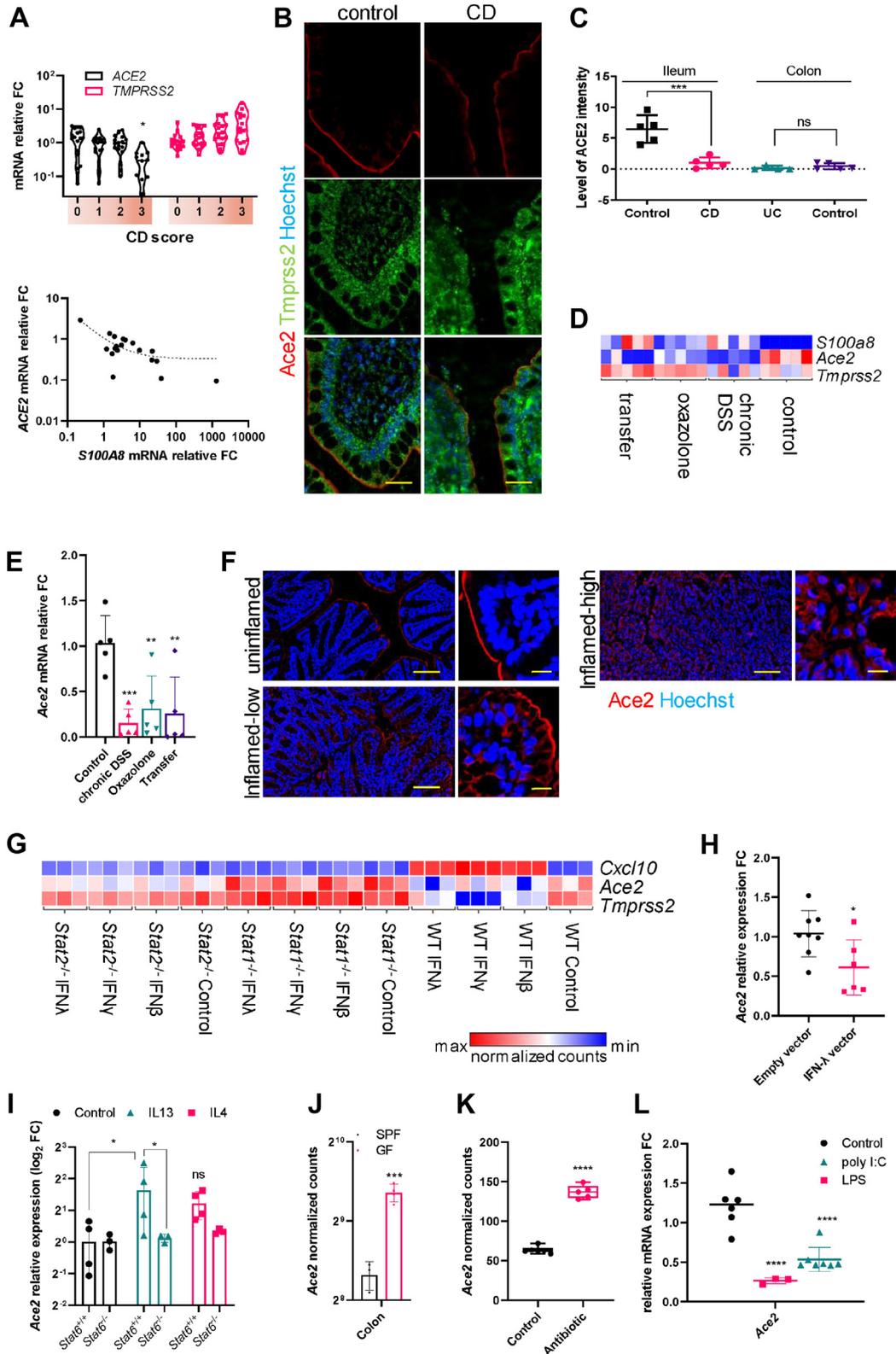
organoids with the IL-13, a key UC type 2 cytokine, showed a significant upregulation of *Ace2* but not *Tmprss2* transcripts (Figure 1*I*). Of note, such upregulation was absent in organoids from mice lacking *Stat6* (Figure 1*I*). Collectively, these data indicate that IEC *Ace2* is regulated reciprocally by IL-13:STAT6 versus IFN:STAT1 signaling.

Immense person-to-person variation is reported for COVID-19, and the composition of gut microbiota, among other factors, could account for this. Interestingly, germ-free mice showed a 2-fold increase in the expression of intestinal *Ace2* versus specific-pathogen-free mice (Figure 1*J*), which was similar to the analysis of 2 previous datasets comparing antibiotic-treated and germ-free mice versus control subjects (Figure 1*K*, Figure S2*A*). Challenging wild-type mice with LPS, a TLR4 agonist, or poly(I:C), a TLR3 agonist, revealed a strong downregulation of intestinal *Ace2* but not *Tmprss2* (Figure 1*L*, Figure S2*B*). Analysis of a previous dataset of germ-free mice monoassociated with *Citrobacter rodentium* also showed similar results (Figure S2*C*). Taken together, our data provide strong evidence that microbial signaling via TLRs regulates intestinal *Ace2*.

Discussion

The spread of COVID-19 to countries with high incidence rates of IBD and recent studies showing SARS-CoV-2's ability to infect gastrointestinal cells have raised concerns on the severity of COVID-19 in IBD patients. A crucial yet poorly known aspect is the understanding of how the SARS-CoV-2 receptors are regulated on IEC. In this regard, we first found that CD differed from UC in which the expression of *ACE2* was repressed in inflamed CD but not UC tissues. Interestingly, *Ace2* was repressed in murine colitis models where Type 1 cytokines predominate, whereas UC involves a Type 2–like immune response. Our study showed that IEC *Ace2* is regulated differentially based on the predominant cytokine response and stage of inflammation highlighting the need for further investigation.

Interestingly we found that *Ace2* but not of *Tmprss2* mRNA expression correlated with the presence of gut microbiota with a strong negative correlation in various mouse models

and publicly available datasets. Whether such regulation of *ACE2*, via commensal flora, also occurs in human IEC is still to be determined. It is tempting to speculate that the composition of commensal microbiota is linked to the individual differences in COVID-19 susceptibility. Our findings suggest that treatment with antibiotics could influence the expression levels of mucosal *ACE2* and alter the susceptibility of IEC to be infected by the SARS-CoV-2. Overall, our study uncovers novel regulatory effectors of IEC *ACE2* that impact its expression in IBD. Our data indicate that the large surface area of the gut may act as an amplifier of SARS-CoV-2.

Supplementary Material

References

1. Ding Q, et al. J Med Virol 2020;92:1549–1555.
2. Pan Y, et al. Eur Radiol 2020;30:3612–3613.
3. Wang D, et al. JAMA 2020;323:1061–1069.
4. Zhu N, et al. N Engl J Med 2020;382:727–733.
5. Hoffmann M, et al. Cell 2020;181:271–280.
6. Pan L, et al. Am J Gastroenterol 2020;115:766–773.
7. Lamers MM, et al. Science 2020;369:50–54.
8. Garg M, et al. J Ren Angioten Aldost Syst 2015;16:559–569.

Correspondence
Address correspondence to: Christoph Becker, PhD, Department of Medicine 1, Friedrich-Alexander-University Erlangen-Nuremberg, Erlangen, 91052, Germany. e-mail: christoph.becker@uk-erlangen.de.

Figure 1. (*A*) Relative mRNA expression levels from ileal biopsies of CD patients at various disease severity scores and the correlation of expression levels of *S100A8* and *ACE2* (11–18 per group $P < .05$ vs Score 0). (*B*) Immunostaining for ACE2 and TMPRSS2 from the ileum of uninflamed and inflamed gut tissues from CD patients and (*C*) the quantification of ACE2 staining intensities. Scale bar = 50 μm (4–5 per group $P < .001$ vs control). (*D*) Heatmap of log2-transformed reads per kilobase of transcript, per million mapped reads (RPKM) values for the indicated genes in various models of experimental colitis and (*E*) the relative quantitative polymerase chain reaction (qPCR) mRNA expression levels of *Ace2* from the same samples (5 per group P **$<.01$, ***$<.001$ vs control). (*F*) Immunostaining of ACE2 in control and Dextran sulfate sodium (DSS)-treated (inflamed) mouse tissues. Scale bar = 150 μm, inset 20 μm. (*G*) Heatmap of log2-transformed RPKM values for the indicated genes from small intestinal organoids derived from C57/Bl6 (WT), *Stat1* or *Stat2* sufficient (+/+) or deficient (-/-) mice for the indicated IFN treatments. (*H*) Relative qPCR mRNA expression levels of *Ace2* from the small intestine of mice that were injected with indicated expression vectors (6–8 per group $P < 0.05$). (*I*) Relative qPCR mRNA expression levels of *Ace2* from small intestinal organoids of *Stat6* sufficient (+/+) and deficient (-/-) mice stimulated with IL-13 or IL-4 versus control subjects (3–4 per group $P < .05$, ns = not significant). (*J*) Normalized counts (RPKM) for *Ace2* from germ-free (GF) versus specific pathogen-free (SPF) mice (3 per group $P < .001$). (*K*) Analysis of normalized mRNA counts of *Ace2* expression from the dataset GDS3921 of mice treated with antibiotics to deplete microbiota. (*L*) Relative qPCR mRNA expression levels of *Ace2* from the small intestine of mice treated either with LPS or with poly(I:C) versus respective control subjects (3–7 per group P ****$<.0001$ vs control).

Barbara Ruder,[1] Ingo Ganzleben,[1] Claudia Günther,[1] David Voehringer,[8] Sebastian Zundler,[1,5] Markus F. Neurath,[1,3,5] and Britta Siegmund[2,3]

CRediT Authorship Contributions

Jay Vasant Patankar, PhD (Conceptualization: Equal; Data curation: Equal; Formal analysis: Equal; Project administration: Equal; Supervision: Equal; Visualization: Equal; Writing – original draft: Lead; Writing – review & editing: Equal). Mircea Chiriac, PhD (Conceptualization: Equal; Formal analysis: Equal; Funding acquisition: Equal; Methodology: Equal; Project administration: Equal; Writing – review & editing: Equal). Malte Lehmann, MD (Data curation: Equal; Formal analysis: Equal; Methodology: Equal). Anja A. Kühl, PhD (Conceptualization: Equal; Data curation: Equal; Formal analysis: Equal; Investigation: Equal; Methodology: Equal; Writing – review & editing: Equal). Raja Atreya, MD PhD (Conceptualization: Equal; Funding acquisition: Equal; Project administration: Equal; Supervision: Equal; Writing – review & editing: Equal). Christoph Becker, PhD, Prof. Dr. rer. nat. (Conceptualization: Equal; Funding acquisition: Lead; Supervision: Lead; Writing – review & editing: Equal).

Conflicts of interest

The authors disclose no conflicts.

Funding

Supplementary Materials and Methods

Patients and controls

Intestinal biopsies or gut specimens from IBD patients [n= 129; similar gender representation, 18–71 years] were used for RNA isolation [n= 113, of varying degrees of inflamed and non-inflamed control tissue] and immunohistochemical staining [n = 16] of paraffin sections. For analysis of coexpression, CD (ileum): 5 male, 1 female (3 low-grade, 3 high-grade); 30-58 years; UC (5 colon ascendens, 1 colon transversum): 1 male, 5 female (3 low-grade, 3 high-grade); 31-56 years; and Control (5 Ileum, 5 colon): 2 male, 3 female; 30-68 years were used.

Mice

The generation and maintenance of Stat1, Stat2 and Stat6 knockout mice has been reported before[1]. Housing, breeding, care and experimentation were performed following institutional guidelines approved by the government of Lower Franconia.

Organoid Culture

Based on the method of Sato et al. mouse small intestinal or colon organoids were cultured in Matrigel (BD) domes as described earlier and grown in mouse Intesticult organoid growth medium (Stemcell Technologies, Vancouver, BC). Organoid media were changed every 3-5 days. All experiments were performed in either Advanced DMEM supplemented with predetermined volumes of R-spondin conditioned medium, antibiotics, recombinant mouse EGF, recombinant noggin, B27 supplement and N-Acetylcysteine or in complete mouse Intesticult medium.

Experimental Mouse Colitis Models

The induction of various experimental colitis was performed as previously described[2]. For chronic colitis, mice were challenged with 3 cycles of 1.5% dextran sulfate sodium (DSS) in drinking water interleaved by 2 cycles of normal drinking water. Oxazolone colitis was induced by initially pre-sensitizing the mice by the application of 3% oxazolone solution in an acetone-olive oil delivery solution onto shaved skin. On day 8 post-sensitization, mice were anesthetized and a rectal cannula was instilled to deliver 100μl of the 3% oxazolone solution as enema. T-cell transfer colitis was initiated in mice as described previously[3]. In short, recipient Rag2$^{-/-}$ mice were injected intraperitoneal with isolated and purified T-cells and the course of disease was followed by assessing disease scores for general appearance, body weight, rectal bleeding and stool consistency.

RNA isolation and quantitative real-time PCR

Total RNA from tissues was isolated with the Total RNA kit and from organoids using the microspin total RNA kit (Peqlab Biotechnologies GmbH, Erlangen, Germany) according to the manufacturer's protocol. For tissues 2 μg and for organoids 200ng of total RNA was reverse transcribed using the Script cDNA synthesis Kit (Jena Bioscience GmbH, Jena, Germany). Quantitative real-time PCR was performed on a Roche LightCycler 480 instrument (Roche Diagnostics, Palo Alto, CA) using the QuantiFast^{TM} SYBR® Green PCR Kit (Roche Diagnostics GmbH, Mannheim, Germany). Expression profiles were normalized to the expression levels of the housekeeping genes Gapdh and HPRT1 and associated statistical parameters were analyzed using the 2-$\Delta\Delta$Ct method. Primer sequences:

Mm_Ace2(F-gcagatggctacaactataaccg; R-cctcctcacatagg catgaaga)

Mm_Tmprss2(F-cagtctgagcacatctgtcct; R-ctcggagcata ctgaggca)

Hs_ACE2(F-acagtccacacttgcccaaat; R-tgagagcactgaaga cccatt)

Hs_TMPRSS2(F-gtccccactgtctacgaggt; R-cagacgacgggg ttggaag)

Mm_Gapdh(F-aggtcggtgtgaacggatttg; R- tgtagaccatgtag ttgaggtca)

Hs_HPRT(F- cctggcgtcgtgattagtgat; R- agacgttcagtcctgtc cataa)

Immunofluorescence and Immunohistochemistry

Cryosections were thawed, fixed in 4% PFA, washed, blocked and incubated with anti-TMPRSS2 (abcam, ab92323, 1:100) overnight. Sections were washed and primary antibodies were detected using secondary antibodies and nuclei were counter stained with Hoechst (Thermo Fsicher Scientific GmbH, Erlangen, Germany). Paraformaldehyde fixed, paraffin embedded tissue sections were dewaxed and subjected to antigen retrieval using Tris-EDTA. Tissues were washed, blocked and incubated overnight with anti-ACE2 (Abcam, ab15348, 1:100) followed by washes and detection using labelled secondary antibodies and nuclear counter staining with Hoechst. Images were acquired using the Leica TCS SP5 confocal microscope using appropriate settings. For double staining, paraffin sections were dewaxed and subjected to heat-induced retrieval prior to incubation with primary antibody directed against ACE2 (Abcam, clone EPR4435(2), 1:4000) followed by incubation with peroxidase-labelled secondary antibody employing the EnVision+ System-HRP Labelled Polymer (Agilent). For detection, OPAL670 (Akoya Biosciences) was used. Proteins and enzymes were inactivated (antibody stripping) and sections were incubated with the second primary antibody directed against TMPRSS2 (Abcam clone EPR3861, 1:50,000) followed by incubation with peroxidase-labelled secondary antibody employing the EnVision+ System-HRP Labelled Polymer (Agilent). For detection, OPAL520 (Akoya Biosciences) was used. Nuclei were stained using 4',6-diamidine-2'-phenylindole dihydrochloride (DAPI; Sigma) and sections were coverslipped using Fluoromount G (Southern Biotech). Pictures were acquired by the Zeiss AxioImager Z1 microscope (Carl Zeiss MicroImaging). For analysis, five pictures at 400X magnification of each section were taken in black and white and subjected to gray-scale analysis employing ImageJ (version 1.8.0_112). For the

immunohistochemical detection of ACE2, a heat-induced antigen retrieval at pH 6 was performed. The sections were incubated with primary antibody against ACE2 (Abcam, clone EPR4435(2), 1:1,000) for 30 minutes at room temperature. The primary antibodies were detected using and detected using the EnVision+ System- HRP Labelled Polymer and 3,3'-Diaminobenzidine (DAB, Agilent) was used as chromogen. Sections were counterstained with hematoxylin (Merck Millipore, GmbH, Darmstadt, Germany) and slides were coverslipped with glycerol-gelatine (Merck, GmbH, Darmstadt, Germany).

Analysis of Publicly Available Datasets

For analyzing the gene expression correlations, we used the Gene Expression Omnibus (GEO) through which the following publicly available datasets were obtained GSE16879[4], GSE57533[5], GSE92332[6], GDS4319[7], and GSE71734[8]. Raw expression values were log transformed where applicable. For data sorting and comparison, power query in Microsoft Excel 2016 was used. Datasets were queried for genes of interest and correlation were plotted and calculated using the graphing software GraphPad Prism Ver. 8.0. Raw counts were generated based on Ensemble genes (GENCODE Ver. 26 or Ensemble release 91) with featurecounts, v1.6.4. Analyses were performed using the freely available tools STAR, version 2.7.0d, to map against indexed genomes; and deseq2 version 1.24.0 R package to perform the differential expression analysis.

Statistical Analysis

Analysis of grouped data was performed using two-parameter analyses of variance followed by Dunnett's post hoc-test. Multi-column comparisons were performed using one-way analysis of variance Dunnett's post hoc-test. Comparisons between data sets were performed using Student's t-test. All calculations were performed in Graph-Pad Prism Versions 6.07 and 8.0 and/or Microsoft Excel 2016.

References

1. Shimoda K, van Deursen J, Sangster MY, et al. Lack of IL-4-induced Th2 response and IgE class switching in mice with disrupted Stat6 gene. Nature 1996;380:630–633.
2. Wirtz S, Popp V, Kindermann M, et al. Chemically induced mouse models of acute and chronic intestinal inflammation. Nat Protoc 2017;12:1295–1309.
3. Radulovic K, Ayata CK, Mak'Anyengo R, et al. NLRP6 Deficiency in CD4 T Cells Decreases T Cell Survival Associated with Increased Cell Death. J Immunol 2019; 203:544–556.
4. Arijs I, De Hertogh G, Lemaire K, et al. Mucosal gene expression of antimicrobial peptides in inflammatory bowel disease before and after first infliximab treatment. PLoS One 2009;4:e7984.
5. Abu-Remaileh M, Bender S, Raddatz G, et al. Chronic inflammation induces a novel epigenetic program that is conserved in intestinal adenomas and in colorectal cancer. Cancer Res 2015;75:2120–2130.
6. Haber AL, Biton M, Rogel N, et al. A single-cell survey of the small intestinal epithelium. Nature 2017;551:333–339.
7. El Aidy S, van Baarlen P, Derrien M, et al. Temporal and spatial interplay of microbiota and intestinal mucosa drive establishment of immune homeostasis in conventionalized mice. Mucosal Immunol 2012;5:567–579.
8. Atarashi K, Tanoue T, Ando M, et al. Th17 Cell Induction by Adhesion of Microbes to Intestinal Epithelial Cells. Cell 2015;163:367–380.
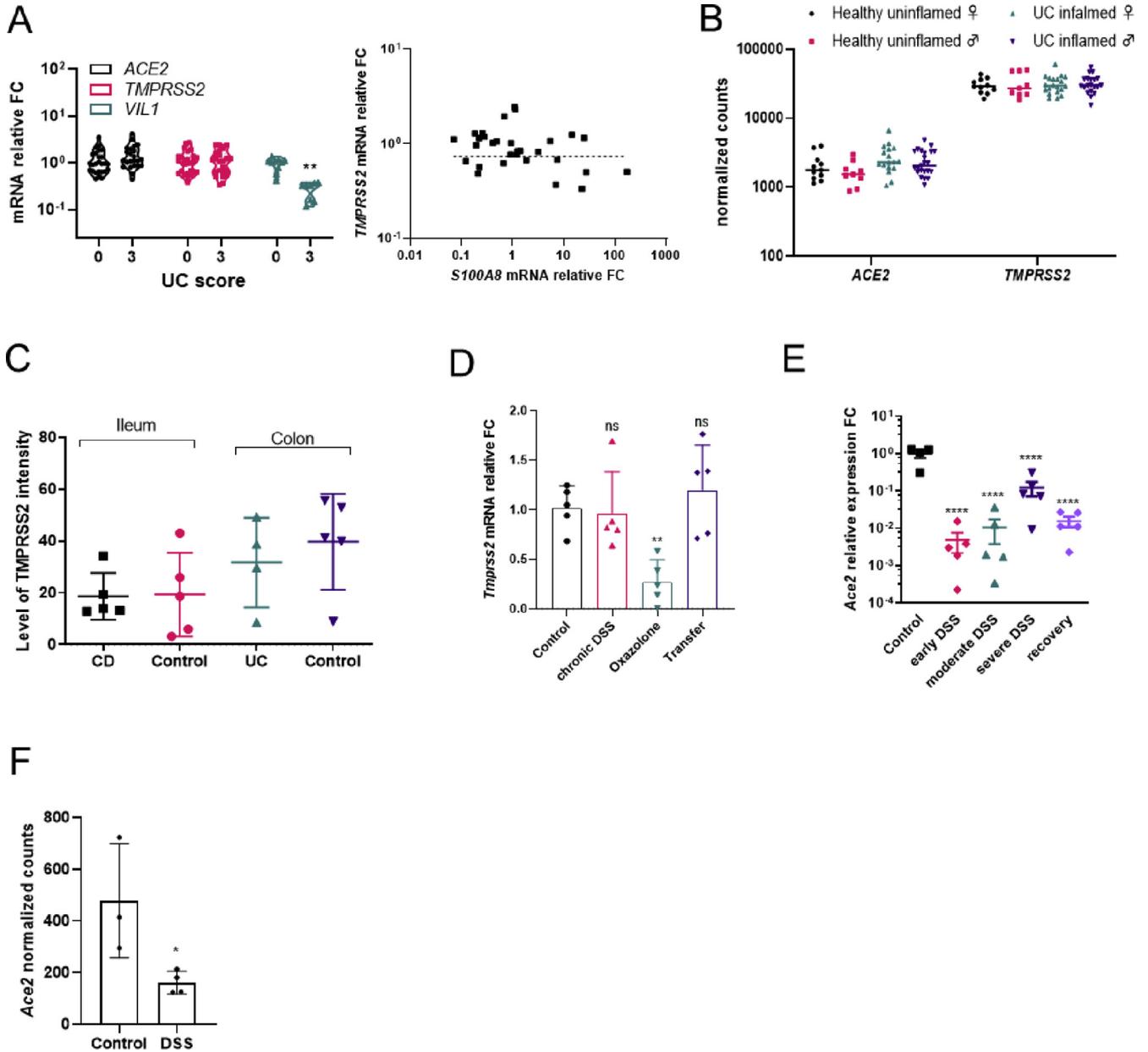
Supplementary Figure 1. (*A*) Relative mRNA expression of indicated genes from colonic biopsies of UC patients at various disease severity scores and the correlation of expression levels of *S100A8* and *ACE2*. (n = 11-18 per group) (*B*) Analysis of colonic genes from the publically available dataset GSE109142 stratified for gender and ulcerative colitis (UC) status. (*C*) Quantification of immunostaining intensities for TMPRSS2 from the ileum and colon of uninflamed and inflamed gut tissues from IBD patients. (*D*) Relative mRNA expression levels (qPCR) of *Tmprss2* from the colons of in various models of experimental colitis (n = 5 per group, p ** < 0.01, ns = not significant) (*E*) Relative mRNA expression levels (qPCR) of *Ace2* from the colons of mice at various stages of DSS colitis. (n = 5 per group, p **** < 0.0001) (*F*) Normalized counts of *Ace2* mRNA expression analyzed from the publically available dataset GSE57533 from DSS treated and control mouse colon tissues (n = 3-4, p * < 0.05).
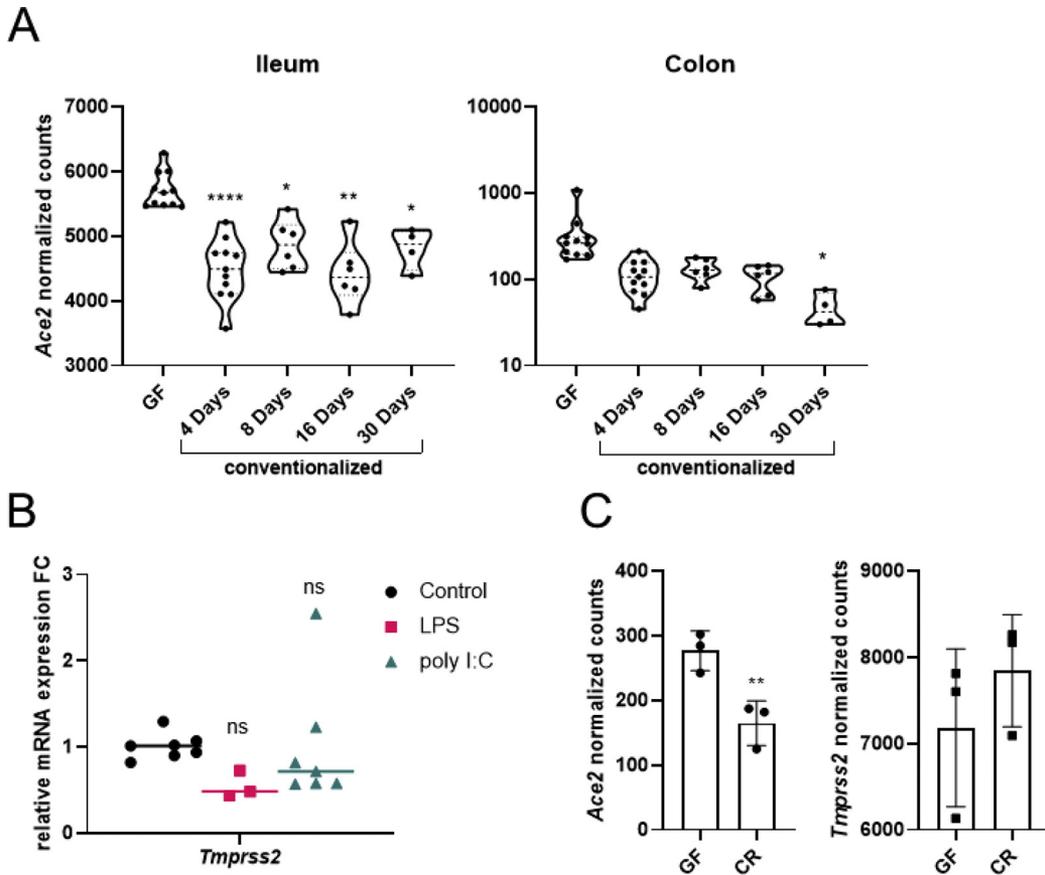
Supplementary Figure 2. (*A*) Analysis of *Ace2* expression in the publicly available dataset GDS4319 from the ileum and the colon of germ free (GF) mice conventionalized for the indicated number of days. (n = 4-11, p *< 0.05, ** < 0.01, **** < 0.0001) (*B*) Relative qPCR mRNA expression levels of *Tmprss2* from the small intestine of mice that were treated either with LPS or with poly(I:C) versus respective controls (n = 3-7, ns = not significant) (*C*) Analysis of *Ace2* and *Tmprss2* expression levels from the publicly available GSE71734 of germfree (GF) mice infected with *Citrobacter rodentium* (CR) bacteria. (n = 3 per group, p ** < 0.01).